Iranian Journal of Chemical Engineering
Vol. 3, No. 3 (Summer), 2006, IAChE

Mathematical modeling of a fixed bed chromatographic reactor for Fischer Tropsch synthesis

*A. Fazeli and M. Kazemeini**
Department of Chemical and Petroleum Engineering, Sharif University of Technology, Tehran, Iran.

Abstract
In this research, Fischer Tropsch synthesis (FTS) has been modeled in the fixed bed chromatographic reactor for the first time by applying a rather complex dispersed plug flow model for fluid phase and linear driving force (LDF) model for adsorbent. Model equations are dynamic, multi-component, non-linear and heterogeneous including reaction and adsorption simultaneously Complex kinetics for FTS and water-gas shift (WGS) reaction and the multicomponent Langmuir adsorption isotherm is used in the model. A set of partial differential and ordinary differential equations with algebraic equations have been converted into a set of ordinary differential equations by using the orthogonal collocation technique. Then this set of equations has been solved by multi-step methods of Numerical Differentiation Formulae (NDF) or Backward Differentiation Formulae (BDF) Known as the Gear's method. Consequently, results for dynamic model and effects of modeling parameters have been analyzed. Through this fixed bed chromatographic reactor model, one may develop a suitable configuration of simulated moving bed chromatographic reactors.

Keywords: *Dynamic Modeling, Fixed Bed Chromatographic Reactors, Adsorption, Fisher Tropsch Synthesis and Orthogonal Collocation*

Introduction
Chromatographic reactors perform chromatographic separation operations based upon adsorption and catalytic reactions by solid particle catalysts in a reactor column, containing a blend of catalyst and adsorber, simultaneously. Reactants and carrier streams are fed into the reactor from the inlet as a fluid phase. Reactions occur during movement of these materials along the reactor column and parts of them are converted into products. The success of these reactors depends on the selective adsorption. Reactants and products' adsorption must be varied enough to achieve a good separation.
FTS has been modeled in fixed bed and slurry bubble column reactors in several works such as [1-6] but it has not been modeled in chromatographic reactors. Also there are some references including modeling of chromatographic reactors and separators in fixed bed and simulated moving bed such as [7-14], but they did not use FTS as their reactions. Because there is no other article pertaining to modeling of FTS in chromatographic reactors, in this work, FTS has been

* Corresponding author:E-mail: kazemini@Sharif.edu

modeled in such reactors for the first time. However, the model was developed under isothermal and unsteady state conditions.
There is a thorough review of these reactors and modeling of them in reference [15]. Here, the FTS and WGS reactions are modeled simultaneously in a chromatographic reactor. Many researchers have investigated modeling of chromatographic separations and different theories with different complexities are presented [16-18]. These theories are based upon adsorption models and discussed in detail elsewhere [16]. A comprehensive review on dynamic and modeling of adsorption and isothermal chromatography is presented by Ruthven [17] where he has divided such models into three classes [17, 18]: equilibrium theory, plate model and rate model. In this research, the rate model with a linear driving force rate expression is used.

Process for modeling

In this section the process has been used for modeling is discussed: the reactor column is taken to be a cylinder with length L and inner diameter D that is packed with catalyst and adsorber. The adsorber selected is Zeolite-5A and the catalyst is determined to be Fe-Cu-K. The feed mixture contains CO, H_2 and carrier gas (He). The feed is passed through the chromatographic reactor. During the reaction, separation through adsorption also occurres. The main reactions are a combination of FTS up to C_2 and WGS:

$$CO + H_2O \longleftrightarrow CO_2 + H_2 \qquad j = 1 \tag{1}$$

$$CO + 3H_2 \longrightarrow CH_4 + H_2O \qquad j = 2 \tag{2}$$

$$2CO + 4H_2 \longrightarrow C_2H_4 + 2H_2O \qquad j = 3 \tag{3}$$

$$2CO + 5H_2 \longrightarrow C_2H_6 + 2H_2O \qquad j = N_R = 4 \tag{4}$$

$$[j] = \begin{bmatrix} 1 \\ 2 \\ 3 \\ 4 \end{bmatrix} \equiv \begin{bmatrix} WGS(1): CO_2\ production \\ FTS1(2): CH_4\ production \\ FTS2(3): C_2H_4\ production \\ FTS3(4): C_2H_6\ production \end{bmatrix} \tag{5}$$

$$\alpha = [\alpha_{ij}] = \begin{bmatrix} -1 & -1 & -2 & -2 \\ 1 & -3 & -4 & -5 \\ 1 & 0 & 0 & 0 \\ -1 & 1 & 2 & 2 \\ 0 & 1 & 0 & 0 \\ 0 & 0 & 1 & 0 \\ 0 & 0 & 0 & 1 \\ 0 & 0 & 0 & 0 \end{bmatrix} \begin{matrix} CO(i=1) \\ H_2(i=2) \\ CO_2(i=3) \\ H_2O(i=4) \\ CH_4(i=5) \\ C_2H_4(i=6) \\ C_2H_6(i=7) \\ He(i=8) \end{matrix} \tag{6}$$

$$\varepsilon_a = \frac{Adsorber\ \ Volume}{Total\ \ Bed\ \ Volume} \tag{7a}$$

$$\varepsilon_b = \frac{Fluid\ \ Volume}{Total\ \ Bed\ \ Volume} \tag{7b}$$

$$\varepsilon_c = \frac{Catalyst\ \ Volume}{Total\ \ Bed\ \ Volume} \tag{7c}$$

Where j is the reaction path number from 1 to N_R and N_R is the total number of reactions. α_{ij} is the stoichiometric coefficient of component i in the reaction path j and volume fraction of adsorber, the fluid and catalyst are ε_a ،ε_b and ε_c , respectively.

Model Assumptions

The main assumptions utilized in this research include:

1- Plug flow with axial dispersion for fluid flow model

2- Isothermal conditions
3- Linear driving force (LDF) approach is adapted for the adsorber
4- Pseudo-homogeneous model for catalytic reactions
5- Fluid velocity is taken to be constant with an average value
6- Pressure drop of the packed bed is taken to be negligible because of low velocity and
7- Langmuir adsorption isotherm is used for multicomponent adsorption equilibrium.

It is noteworthy that, this model is dynamic as it employs the axial dispersion model with linear driving force.

Model Equations

There are two classes of differential equations based upon the above assumptions [15]:

1- Partial mass balance for every component i in the fluid moving through the bed and
2- Linear driving force equation for every component i in the absorber beads

Moreover, there are two classes of algebraic equations including:

1-Reaction kinetics rates and
2-Adsorption equilibrium isotherm equations

All are incorporated into the present model.

Ultimately, developed equations for this model are as follows:

I - Fluid phase (PDEs):

$$\frac{\partial C_{bi}}{\partial t} = -\nu \frac{\partial C_{bi}}{\partial Z} + D_{Li} \frac{\partial^2 C_{bi}}{\partial Z^2} + \frac{\varepsilon_c}{\varepsilon_b} \rho^{cat} \times \sum_{j=1}^{N_R} \alpha_{ij} R_j - \frac{\varepsilon_a}{\varepsilon_b} k_{Ci} \left(\frac{b_i C_{p\infty i} C_{bi}}{1 + \sum_{j=1}^{N_C} b_j C_{bj}} - C_{pi} \right) \quad (8)$$

II - Adsorbent phase (ODEs):

$$\frac{\partial C_{pi}}{\partial t} = k_{Ci} \left(\frac{b_i C_{p\infty i} C_{bi}}{1 + \sum_{j=1}^{N_C} b_j C_{bj}} - C_{pi} \right) \quad (9)$$

III – Related initial and boundary conditions:

I.C.1:

$$t = 0 \quad ; \quad C_{bi} = C_{bi0} = C_{bi}(0, Z) \quad ; \quad 0 < Z \le L \quad (10)$$

I.C.2:

$$t = 0 \quad ; \quad C_{pi} = C_{pi0} = C_{pi}(0, Z) \quad ; \quad 0 \le Z \le L \quad (11)$$

B.C.1:

$$Z = 0 \quad ; \quad \frac{\partial C_{bi}}{\partial Z} = \frac{\nu}{D_{Li}} (C_{bi} - C_{bi,input}) \quad ; \quad t > 0 \quad (12)$$

B.C.2:

$$Z = L \quad ; \quad \frac{\partial C_{bi}}{\partial Z} = 0 \quad ; \quad t > 0 \quad (13)$$

In addition, reactions may be summarized in the following parts:
1- Paraffin formation reactions:

$$nCO + (2n+1)H_2 \longrightarrow C_nH_{2n+2} + nH_2O \qquad (n \ge 1) \quad (14)$$

2- Olefin formation reactions:

$$nCO + 2nH_2 \longrightarrow C_nH_{2n} + nH_2O \qquad (n \ge 2) \quad (15)$$

3- Water gas shift reaction:

$$CO + H_2O \longleftrightarrow CO_2 + H_2 \quad (16)$$

Table 1. Stoichiometric coefficients matrix for FTS and WGS reactions

	Reaction Path					
Reactants	$CO+H_2O$	$CO+3H_2$	$2CO+4H_2$	$2CO+5H_2$	$nCO+2nH_2$	$nCO+(2n+1)H_2$
Products	CO_2+H_2	$CH_4+ H_2O$	$C_2H_4+ 2H_2O$	$C_2H_6+ 2H_2O$	$C_nH_{2n}+n\ H_2O$	$C_nH_{2n+2}+n\ H_2O$
CO	-1	-1	-2	-2	-n	-n
H_2	1	-3	-4	-5	-2n	-(2n+1)
CO_2	1	0	0	0	0	0
H_2O	-1	1	2	2	n	n
CH_4	0	1	0	0	0	0
C_2H_4	0	0	1	0	0	0
C_2H_6	0	0	0	1	0	0
⋮	⋮	⋮	⋮	⋮	⋮	⋮
C_nH_{2n}	0	0	0	0	1	0
C_nH_{2n+2}	0	0	0	0	0	1

FTS and WGS Reaction Rates for Fe-Cu-K catalyst used based upon equations (17)-(20) [19] are presented in the following:

$$R_{CH_4} = \frac{k_{5M} P_{H_2} \alpha_1}{1 + (1 + \frac{1}{K_2 K_3 K_4} \frac{P_{H_2O}}{P_{H_2}^2} + \frac{1}{K_3 K_4} \frac{1}{P_{H_2}} + \frac{1}{K_4}) \sum_{i=1}^{N} (\prod_{j=1}^{i} \alpha_j)} \quad (n = 1) \tag{17}$$

$$R_{C_nH_{2n+2}} = \frac{k_5 P_{H_2} \prod_{j=1}^{n} \alpha_j}{1 + (1 + \frac{1}{K_2 K_3 K_4} \frac{P_{H_2O}}{P_{H_2}^2} + \frac{1}{K_3 K_4} \frac{1}{P_{H_2}} + \frac{1}{K_4}) \sum_{i=1}^{N} (\prod_{j=1}^{i} \alpha_j)} \quad (n \geq 2) \tag{18}$$

$$R_{C_nH_{2n}} = \frac{k_6 (1 - \beta_n) \prod_{j=1}^{n} \alpha_j}{1 + (1 + \frac{1}{K_2 K_3 K_4} \frac{P_{H_2O}}{P_{H_2}^2} + \frac{1}{K_3 K_4} \frac{1}{P_{H_2}} + \frac{1}{K_4}) \sum_{i=1}^{N} (\prod_{j=1}^{i} \alpha_j)} \quad (n \geq 2) \tag{19}$$

$$R_{CO_2} = \frac{k_V (P_{CO} P_{H_2O} / P_{H_2}^{0.5} - P_{CO_2} P_{H_2}^{0.5} / K_P}{1 + K_V P_{CO} P_{H_2O} / P_{H_2}^{0.5}} \tag{20}$$

Partial pressure of component i is calculated based upon the equation (21):

$$P_i = \left(\frac{m_i}{\sum_{i=1}^{N_C} m_i} \right) P_t \tag{21}$$

P_t is the total pressure of the reactor and m_i is the molar flow rate of component i.
α_1 and α_n are calculated from equations (22)-(23):

$$\alpha_1 = \frac{k_1 P_{CO}}{k_1 P_{CO} + k_{5M} P_{H_2}} \quad (n = 1) \tag{22}$$

$$\alpha_n = \frac{k_1 P_{CO}}{k_1 P_{CO} + k_5 P_{H_2} + k_6 (1 - \beta_n)} \quad (n \geq 2) \tag{23}$$

β_n in equation (23) is defined in the following form:

$$\beta_n = \frac{k_{-6}}{k_6} \frac{P_{C_n H_{2n}}}{\alpha_A^{n-1} \frac{k_1 P_{CO}}{k_1 P_{CO} + k_5 P_{H_2}} + \frac{k_{-6}}{k_1 P_{CO} + k_5 P_{H_2} + k_6} \sum_{i=2}^{n} (\alpha_A^{i-2} P_{C_{n-i+2} H_{2(n-i+2)}})} \tag{24}$$

$(n \geq 2)$

α_A in equation (24) is defined in equation (25):

$$\alpha_A = \frac{k_1 P_{CO}}{k_1 P_{CO} + k_5 P_{H_2} + k_6} \tag{25}$$

Reaction rate constants are changed with temperature according to the Arrhenius equation:

$$k_i(T) = k_{i,0} \exp(\frac{-Ei}{RT}) \tag{26}$$

Optimum values for reaction rate parameters are summarized in table 2 [19]:

Equilibrium constant for the WGS reaction is estimated based upon equation (2۷) as a function of temperature [19]:

$$\ln(K_P) = \frac{5078.0045}{T} - 5.8972089 + (13.958689 \times 10^{-4}) T - (27.592844 \times 10^{-8}) T^2 \tag{27}$$

Multicomponent adsorption parameters of the Langmuir isotherm are given from reference [20]. The Langmuir isotherm is implemented as:

$$\frac{q_i^{*eq}}{q_{\infty i}} = \frac{b_i' P_i}{1 + \sum_{j=1}^{N_C} b_i' P_i} \tag{28}$$

Table 2. FTS and WGS reactions rates parameters [19]

Parameter	Dimension	Values	t-student dispersion
k_1	mole gr^{-1} s^{-1} bar^{-1}	(2.23+0.28) $\times 10^{-5}$	15.32
$k_{5M,0}$	mole gr^{-1} s^{-1} bar^{-1}	(4.65+0.29) $\times 10^{3}$	30.50
E_{5M}	kJ mole^{-1}	(9.289+0.094) $\times 10^{1}$	198.35
$k_{5,0}$	mole gr^{-1} s^{-1} bar^{-1}	(2.74+0.12) $\times 10^{2}$	44.26
E_5	kJ mole^{-1}	(8.701+0.083) $\times 10^{1}$	206.27
$k_{6,0}$	mole gr^{-1} s^{-1}	(2.23+0.28) $\times 10^{-5}$	8.87
E_6	kJ mole^{-1}	(1.1104+0.0213) $\times 10^{2}$	102.01
$k_{v,0}$	mole gr^{-1} s^{-1} bar$^{-1.5}$	(1.57+0.022) $\times 10^{1}$	142.32
E_v	kJ mole$^{-1(}$	(4.508+0.149) $\times 10^{1}$	59.37
k_{-6}	mole gr^{-1} s^{-1} bar^{-1}	(2.75+0.25) $\times 10^{-5}$	21.50
K_V	bar$^{-0.5}$	(1.13+0.08) $\times 10^{-3}$	28.28
K_2	-	(1.81+0.16) $\times 10^{-2}$	21.89
K_3	-	(4.68+0.66) $\times 10^{-2}$	13.89
K_4	-	(2.26+1.02) $\times 10^{-1}$	4.35

Dimensionless Equations

Dimensionless variables and parameters are defined in the following manner:

a. dimensionless independent variables:

$$\bar{t} = \frac{u\,t}{L\varepsilon_b} = \frac{\nu\,t}{L} \tag{29}$$

$$\bar{Z} = \frac{Z}{L} \tag{30}$$

b. dimensionless dependent variables:

$$\bar{Y}_{bi} = \frac{C_{bi}}{C_{br}} \tag{31}$$

$$\bar{Y}_{pi} = \frac{C_{pi}}{C_{pr}} \tag{32}$$

c. dimensionless parameters:

$$\alpha = -1 \tag{33}$$

$$\beta_i = \frac{D_{Li}}{L\nu} = \frac{\varepsilon_b D_{Li}}{Lu}\frac{1}{Pe_{Li}} \tag{34}$$

$$\gamma_i(\bar{Y}_{pj}, \bar{Y}_{bj}\ s) = \frac{\varepsilon_c \rho^{cat}}{\varepsilon_b \nu\, C_{br}} \times \sum_{j=1}^{N_R} \alpha_{ij} R_j - \frac{\varepsilon_a C_{pr}}{\varepsilon_b C_{br}} \times \lambda_i(\bar{Y}_{pj}, \bar{Y}_{bj}\ s) \tag{35}$$

$$\lambda_i(\overline{Y}_{pj},\overline{Y}_{bj}\ s)=\frac{k_{Ci}L}{C_{pr}\nu}\left(\frac{b_iC_{p\propto i}\overline{Y}_{bi}C_{br}}{1+C_{br}\sum_{j=1}^{N_C}b_j\overline{Y}_{bj}}-\overline{Y}_{pi}C_{pr}\right) \quad (36)$$

$$\overline{Y}_{bi0}=\frac{C_{bi0}}{C_{br}} \quad (37)$$

$$\overline{Y}_{pi0}=\frac{C_{pi0}}{C_{pr}} \quad (38)$$

$$\overline{Y}_{bi,input}=\frac{C_{bi,input}}{C_{br}} \quad (39)$$

Dimensionless equations are summarized in the following:

PDEs :

$$\left(\frac{\partial\overline{Y}_{bi}}{\partial\bar{t}}\right)=\alpha\left(\frac{\partial\overline{Y}_{bi}}{\partial\overline{Z}}\right)+\beta_i\left(\frac{\partial^2\overline{Y}_{bi}}{\partial\overline{Z}^2}\right)+\gamma_i(\overline{Y}_{pj},\overline{Y}_{bj}\ s) \quad (40)$$

$$ODEs: \quad \frac{\partial\overline{Y}_{pi}}{\partial\bar{t}}=\lambda_i(\overline{Y}_{pj},\overline{Y}_{bj}\ s) \quad (41)$$

$$I.C.1: \quad \bar{t}=0 \quad ; \quad \overline{Y}_{bi}=\overline{Y}_{bi0} \quad (42)$$

$$I.C.2: \quad \bar{t}=0 \quad ; \quad \overline{Y}_{pi}=\overline{Y}_{pi0} \quad (43)$$

$$B.C.1: \quad \overline{Z}=0 \quad ; \quad \frac{\partial\overline{Y}_{bi}}{\partial\overline{Z}}=\frac{1}{\beta_i}\left(\overline{Y}_{bi}-\overline{Y}_{bi,input}\right) \quad (44)$$

$$B.C.2: \quad \overline{Z}=1 \quad ; \quad \frac{\partial\overline{Y}_{bi}}{\partial\overline{Z}}=0 \quad (45)$$

i is a component number index between 1 and N_c which is equal to 8.

Solution by Orthogonal Collocation Method [15, 21-28]

Roots of Jacobean polynomial are applied for collocation points. Lagrange interpolation is used. Based on the orthogonal collocation method, position derivatives are formulated from the interpolated polynomial and based on the method of lines these are substituted into the partial differential equations (PDEs) to convert them to the ordinary differential equations (ODEs). Boundary conditions are applied in these equations. Algebraic equations of adsorber equilibriums and reactions rates are introduced into this equation. Two dimensional matrixes of variables are converted to a vector of variables by a one by one correspondence equation. A set of ODEs has been solved by multistep methods of numerical differentiation formulae (NDF) or backward differentiation formulae (BDF), known as the Gear's method. ODEs solving is down by MAT LAB [29] software.

Results and Discussions

There are FTS chromatographic experimental results, only in Pakseresht's work [30]. Thus, results of this research are compared with those of Pakseresht's in Fig. 1. Related trends are in good agreement but there are differences in absolute values between the present model predictions and his experimental data. This might be due to a different kinetic rates of the catalyst utilized in Pakseresht's work [30] which is different to the Wang et al. work [19]. Furthermore, Pakseresht's catalysts are not experimentally tested for determining rate expressions or fitting kinetic parameters.

Some other model parameters are summarized in table 3. The model is solved by orthogonal collocation and the results of this run are indicated in Fig. 2a-e as an example.

In Fig. 2a, dimensionless concentrations of CO, H_2, CO_2 & H_2O in the chromatographic reactor bed vs. the dimensionless length of the reactor and dimensionless time are indicated. CO and H_2 are consumed along the

chromatographic reactor. Therefore, the concentrations of them are reduced while z is increased from zero to one. The chromatographic reactor bed is full of He at start up, so CO and H_2 concentrations in the bed is zero along the chromatographic reactor at zero time. Over a period of time, CO and H_2 concentrations in the bed at the inlet of the chromatographic reactor is changed corresponding to the unit step function. And then when more time has elapsed, their concentration profiles along the chromatographic reactor axis does not change significantly. This is the steady state time. If planes of z equal to one, are interfered to these three dimensional plots, breakthrough curves of outlet concentrations are obtained. These curves are "S" shaped. H_2O is a byproduct of hydrocarbon products and is consumed with CO in a water-gas-shift reaction to produce H_2 and CO_2. water-gas-shift reaction in Fe catalysts progresses more than CO catalysts. But Fe catalysts are cheaper than CO catalyst. In this research Fe-Cu-K catalyst has been used, so water-gas-shift reaction progresses and water is converted to CO_2. Therefore water concentrations are less than CO_2 concentrations, and this matter is led to reduction in deactivation of Fe catalyst by water. There is not any CO_2 & H_2O in the fresh feed. Therefore, the concentrations of them are equal to zero at the inlet of the reactor. At the initial time, the bed is full of carrier gas, so the concentrations of CO_2 & H_2O are zero. Along the z-axis, they are produced and the concentrations of them are increased. Adsorption of CO, H_2 is less than CO_2 & H_2O, therefore CO, H_2 have left the reactor before CO_2 & H_2O. Adsorption together with reaction, decreases water concentration all along the reactor. Therefore, Fe catalyst deactivation is reduced.

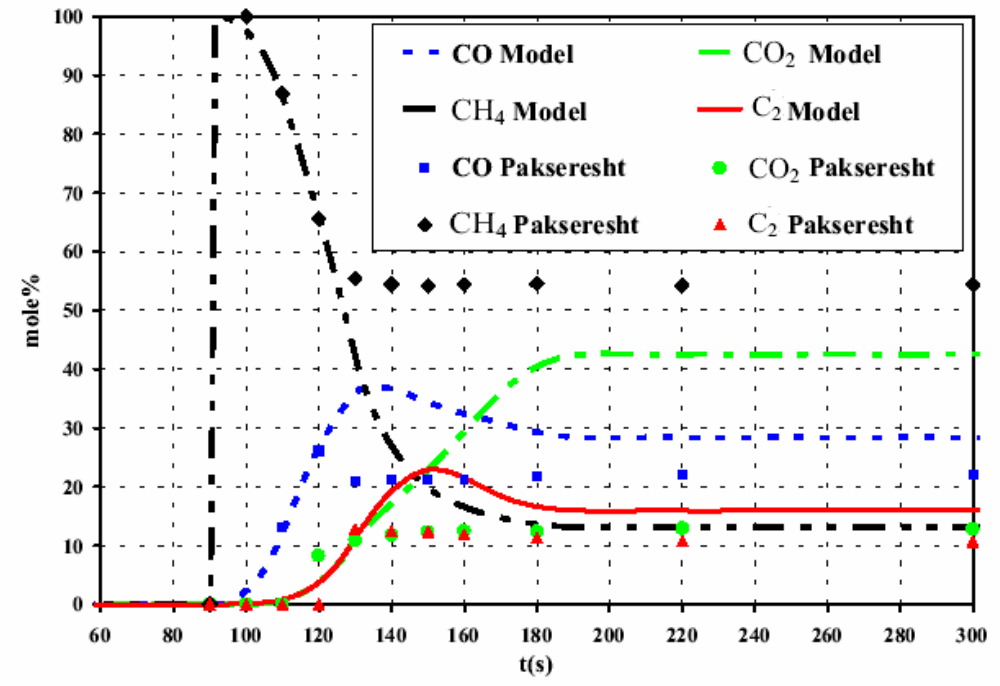

Fig 1. Comparison of present model and experimental results of Paksereshт

Table 3. Data that are used for model in Fig. 2a-e

Parameter	Value	Dimension	Description
ε_a	0.2	-	Adsorber volume fraction
ε_b	0.6	-	Fluid volume fraction
ε_c	0.2	-	Catalyst volume fraction
Y_F He	0.566	-	Carrier gas dimensionless concentration in feed
Y_F CO	0.189	-	Carbon monoxide dimensionless concentration in feed
Y_F H_2	0.245	-	Hydrogen dimensionless concentration in feed
ε_p	0.31	-	Adsorbent porosity is used for k_{Ci} correlation
Rp	1	mm	Catalyst radius
T	280	^{0}C	Temperature
P	18	Bar	Pressure
L	53	Cm	Column length
D	2	Cm	Column diameter
N_{total}	22	-	Total no. of collocation points
Alpha	0	-	Jacobean polynomial parameter
Beta	0	-	Jacobean polynomial parameter
Cpr	1.9762	kmole/m3	Reference concentration of the adsorber particle
Cbr	0.2215	kmole/m3	Reference concentration of the bed
v	0.009	m/s	Superficial velocity

Fig. 2b, contains four plottings of dimensionless concentration of CH_4, C_2H_2, C_2H_6 & He in the chromatographic reactor bed vs. the dimensionless length of the reactor and dimensionless time.

CH_4, C_2H_2 and C_2H_6 are products. They are produced along the chromatographic reactor axis. Ethylene production is more than ethane production and this is good for ethylene production that is one of the important petrochemical feeds. The bed of the chromatographic reactor is full of He at initiatial time, so the carrier gas concentration is at a maximum level at t is equal to zero. The concentration of it is reduced to a minimum level and fixed to fresh feed concentration at steady state time. Methane production is not suitable, because it must be converted to syn. gas again. Catalyst kinetics dictates the production of methane, but adsorption helps to separate it in a simulated moving bed chromatographic reactor because of methane spillage at the outlet of the reactor before steady state time.

Fig. 2c, indicates three dimensional plots of dimensionless concentration of CO, H_2, CO_2 & H_2O in adsorber particles vs. the dimensionless length of the reactor and dimensionless time. Concentrations in the adsorber particles follow the concentrations in the chromatographic reactor bed. Increasing concentrations in the chromatographic reactor bed increases the adsorption driving force and increases concentrations in the adsorber particles. H_2 concentrations in adsorbent vs. time in a constant z have a maximum. These maximums are dealt with competetive adsorption. CO_2 & H_2O concentrations in adsorber particles are increased along the z-axis. Not all the bed becomes full of adsorbed materials because the carrier gas enters with the feed constantly.

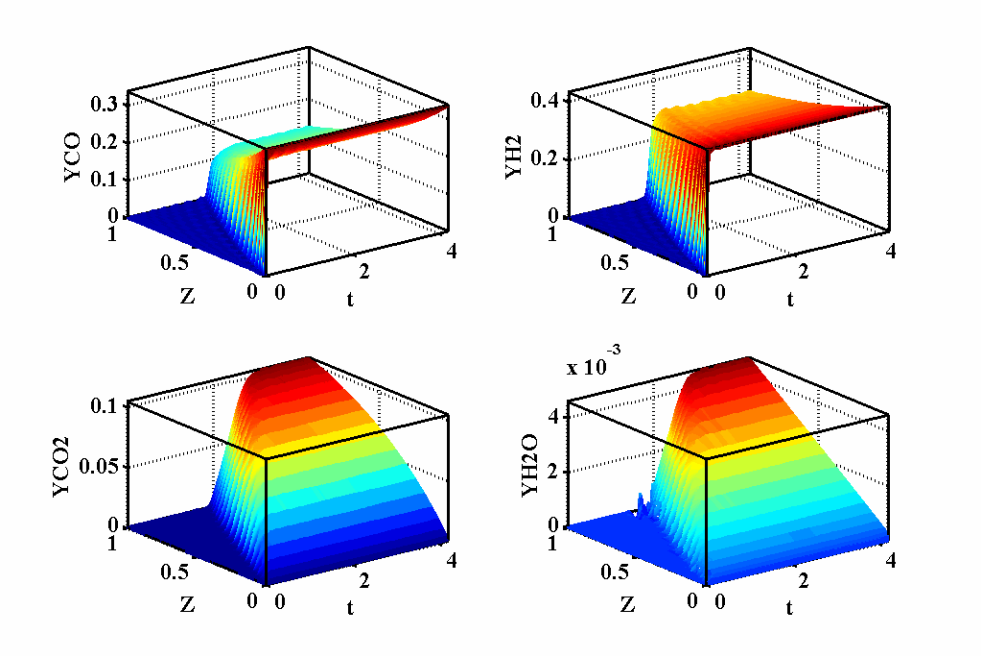

Fig 2a. Dimensionless concentration of CO, H_2, CO_2 & H_2O in the chromatographic reactor bed vs. dimensionless length of the reactor and dimensionless time

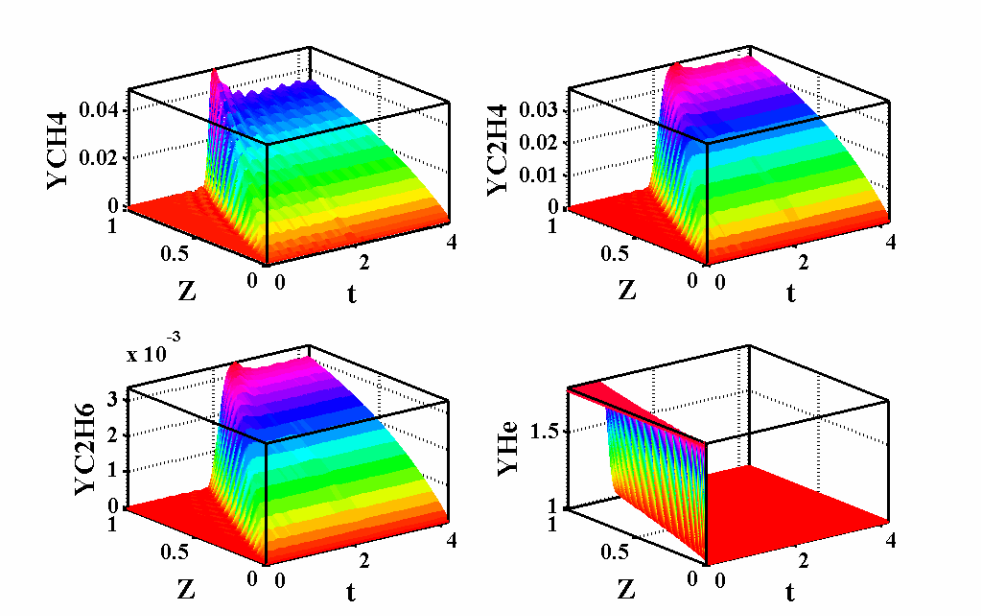

Fig 2b. Dimensionless concentration of CH_4, C_2H_4, C_2H_6 & He in the chromatographic reactor bed vs. dimensionless length of the reactor and dimensionless time

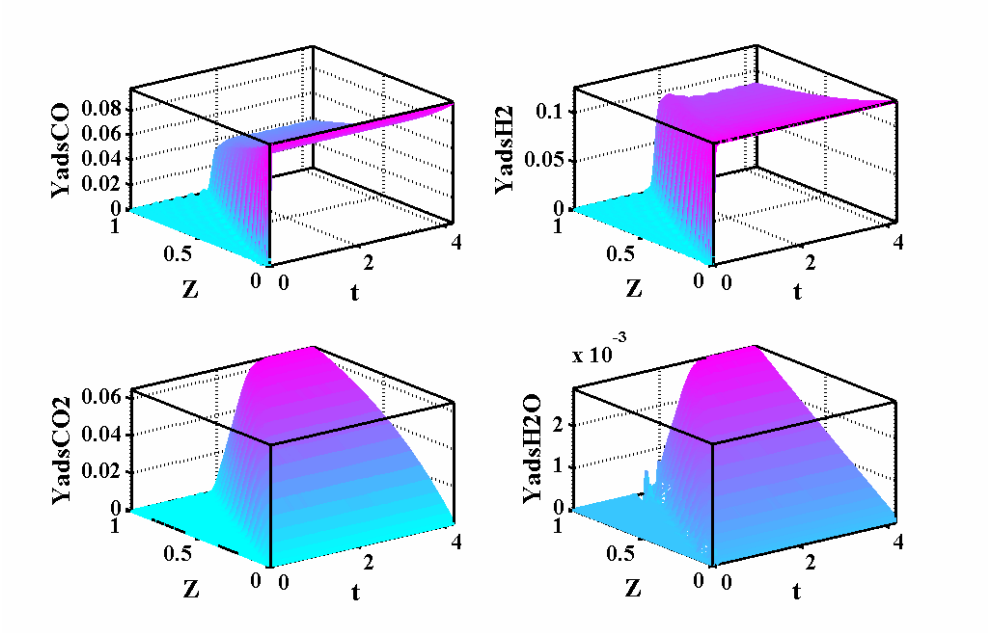

Fig 2c. Dimensionless concentration of CO, H_2, CO_2 & H_2O in the adsorber particles vs. dimensionless length of the reactor and dimensionless time

In Fig. 2d, dimensionless concentration of CH_4, C_2H_4, C_2H_6 & He in the adsorber particles vs. dimensionless length of the reactor and dimensionless time have been plotted. CH_4, C_2H_4 and C_2H_6 concentrations in the adsorber vs. time in a constant z have maximums. These maximums are dealt with competetive adsorption. The carrier gas, He, does not adsorb.

Mole fractions of some components in the outlet of the chromatographic reactor vs. time have been indicated in two dimensional plots of Fig. 2e. In this chromatographic reactor, upon entering the feed, during the reaction and producing the products, compo-nents are separated, because of differences in adsorption selectivity. As Fig. 2e indicates, carbon monoxide and methane exit from the reactor, earlier than carbon dioxide and ethylene. This means that the outlet stream of the FTS chromatographic reactor can be divided into two main streams: one stream contains lighter components (methane and carbon monoxide) and the other stream contains heavier components (carbon dioxide and ethylene). This is the main idea for developing simulated moving bed chromato-graphic reactors for reaction and adsorption simultaneously and continuously.

Conclusions

The fixed bed chromatographic reactor has been modeled for FTS and WGS reactions. The model equations have been solved numerically by the orthogonal collocation method. The trends of the present model predictions and experimental results are in good agreement. Differences between these absolute values might be attributed to the catalyst kinetics which is not the same for both cases. Implementing the axial dispersion model and incorporating the linear driving force approach for the adsorber, resulted in simplicity of the model and a suitable speed for numerical solution. The orthogonal collocation method is suitable for the numerical solution of this model. The model can predict the maximum in breakthrough curves because of competitive adsorption. The model has been run for different conditions and the main conclusions are summarized as follows:

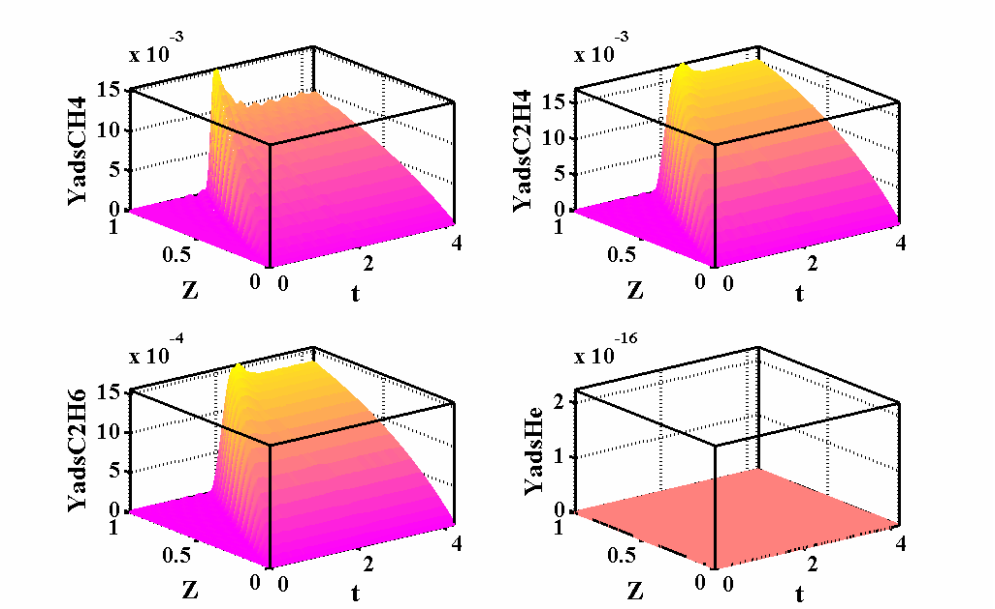

Fig 2d. Dimensionless concentration of CH_4, C_2H_4, C_2H_6 & He in adsorber particles vs. dimensionless length of chromatographic reactor and dimensionless time

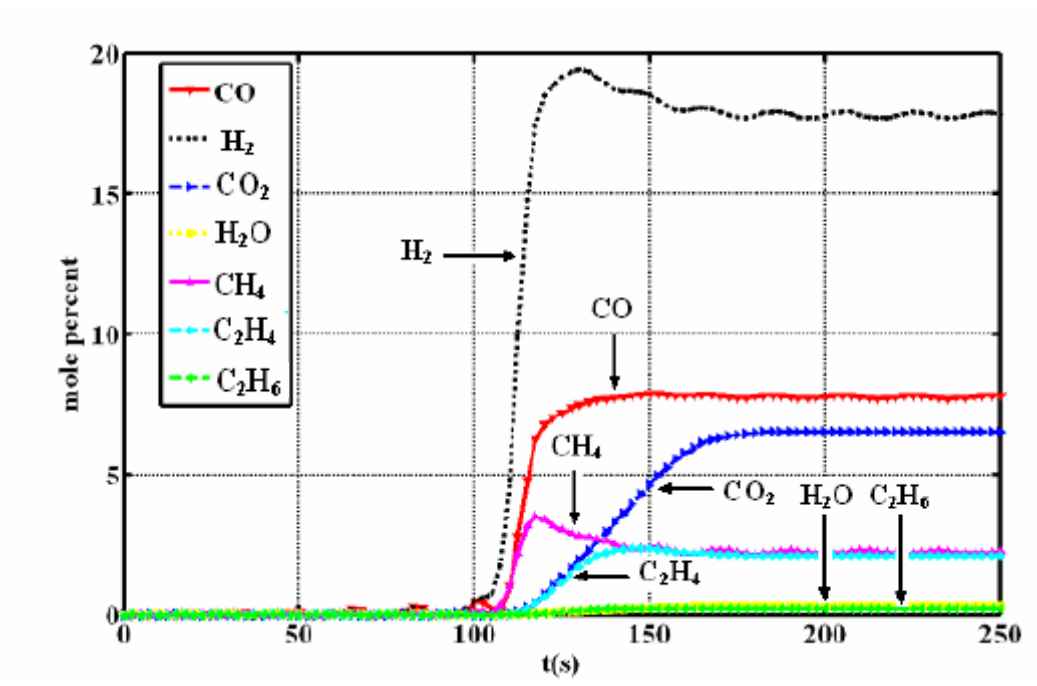

Fig 2e. Mole fractions of some components in outlet of the chromatographic reactor vs. time

1-Increasing the temperature can increase the reaction rates and decrease the adsorption rates. Therefore, there is an optimum temperature. In this temperature, suitable adsorption with good reaction progress can be obtained.

2-Increase in pressure is suitable for reaction-adsorption and is contrary to desorption.

3-Increasing of the volume fraction of absorber advantages the separation.

4-Reduction in average velocity and increase in reactor length, increases the reaction and adsorption rates, because the residence time increases.

5-By increasing the volume fraction of carrier gas, separation rates are increased and reaction rates are decreased.

The fixed bed chromatographic reactor model developed in this work may be extended to simulate moving bed chromatogramphic reactors. Therefore, this research presents the basic steps to develop a mathematical model and numerical solution of model equations for a complex reaction and separation phenomenon to be optimized for such important methane conversion processes.

References

1. Wang, Y. N., Xu, Y. Y., Li, Y. W., Zhao, Y. L., and Zhang, B. J., "Heterogeneous modeling for Fixed bed Fischer Tropsch synthesis: Reactor model and its applications", Chem. Eng. Sci., **58** (3-6), 867 (2003).
2. Rados, N., Al-Dahhan, M. H., and Dudukovic, M. P., "Modeling of the Fischer Tropsch synthesis in slurry bubble column reactors," Cat. Today, **79–80**, 211 (2003).
3. Ahon, V. R., E. F., Costa., Monteagudo, J. E. P., Fontes, C. E., Biscaia, E. C., and Lage, P. L. C., "A comprehensive mathematical model for the Fischer Tropsch synthesis in well-mixed slurry reactors," Chem. Eng. Sci., **60** (3), 677 (2005).
4. Deckwer, W. D., Serpeman, Y., Ralek, M., and Schmidt, B., "Modeling the Fischer Tropsch synthesis in the slurry phase," Ind. Eng. Chem. Process Des. & Dev., **21**, 231 (1982).
5. Saxena, S. C., Rosen, M., Smith, D. N., and Ruether, J. A., "Mathematical modeling of Fischer Tropsch slurry bubble column reactors," Chem. Eng. Commu., **40**, 97 (1986).
6. Maretto, C., and Krishna, R., "Modeling of a bubble column slurry reactor for Fischer Tropsch synthesis," Cat. Today, **52** (2-3), 279 (1999).
7. Pilgrim, A., Kawase, M., Matsuda, F., and Miura, K., "Modeling of the simulated moving-bed reactor for the enzyme-catalyzed production of lactosucrose," Chem. Eng. Sci., **61** (2), 353 (2006).
8. Yu, W., Hidajat, K., and Ray, A. K., "Optimization of reactive simulated moving bed and varicol systems for hydrolysis of methyl acetate," Chem. Eng. J., **112** (1-3), 57 (2005).
9. Haaga J., Vande Wouwera, A., Lehoucq, S., and Saucez, P., "Modeling and simulation of a SMB chromatographic process designed for enantio separation," Control Eng. Prac., **9**, 921 (2001).
10. Klatt, K. U., Dunnebier, G., and Engell, S., "Modeling and computationally efficient simulation of chromatographic separation processes," Math. & Comp. Sim., **53** (4-6), 449 (2000).
11. Zhang H., and Cheng D., "Mathematical model for a fixed bed adsorptive reactor," Carbon, **38** (6), 877 (2000).
12. Dunnebier, G., and Klatt, K. U., "Modeling and simulation of nonlinear chromatographic separation processes: a comparison of different modeling approaches," Chem. Eng. Sci., **55** (2), 373 (2000).
13. Pais, L. S., Loureiro, J. M., and Rodrigues A. E., "Modeling, simulation and operation of a simulated moving bed for continuous chromatographic separation of 1,1-bi-2-naphthol enantiomers," J. Chrom. A, **769** (1), 25 (1997).
14. Kruglov, A., Bjorklund, M. C., and Carr, R.

W., "Optimization of the simulated countercurrent moving bed chromatographic reactor for the oxidative coupling of methane," Chem. Eng. Sci., **51** (11), 2945 (1996).

15. Fazeli, A., Mathematical modeling of hybrid process between Fischer Tropsch synthesis (FTS) catalytic reaction and separation by adsorption in a simulated moving bed reactor (SMBR), MSc. Thesis, Sharif University of Technology (2004).
16. Do, D.D., Adsorption analysis: equilibria and kinetics, 1st ed., Imperial College Press, London (1998).
17. Ruthven, D. M., Principles of adsorption and adsorption processes, 1st ed.,Wiley, New York (1984).
18. Gu, T., Mathematical modeling and scale up of liquid chromatography, Springer, Berlin (1995).
19. Wang, Y. N., Ma, W. P., Lu, Y. J., Yang, J. , Xu, Y. Y., Xiang, H. W., Li, Y. W., Zhao, Y. L., and Zhang, B. J., "Kinetics modeling of Fischer–Tropsch synthesis over an industrial Fe–Cu–K catalyst," Fuel, **82** (2), 195 (2003).
20. Pakseresht, S., Kazemeini, M., and Akbarnejad, M., "Equilibrium isotherms for CO, CO_2, CH_4 and C_2H_4 on the 5A molecular sieve by a simple volumetric apparatus," Sep. & Purif. Tech., **28** (1), 53 (2002).
21. Rice, G. R., and Do, D. D., Applied mathematics and modeling for chemical engineers, 1st ed., John Wiley & Sons Inc., pp.592-615 (1995).
22. Finlayson B. A., Non-linear analysis in chemical engineering, 1st ed., McGraw-Hill Inc., pp.191-214,231-245 (1980).
23. Finlayson B. A., The method of weighted residuals and variational principles, with application in fluid mechanics, heat and mass transfer, 1st ed., Academic Press Inc., London, pp. 126-129 (1972).
24. Desai C.S., Elementary finite element method, 1st ed., Prentice-Hall Inc., New Jersey, pp. 202-210 (1979).
25. Constantinides A., and Mostoufi N., Numerical methods for chemical engineers with MATLAB applications, 1st ed., Prentice-Hall Inc., New Jersey (1999).
26. Gerald, C. F., and Wheatley, P. O., Applied numerical analysis, 6th ed., Addison-Wesley, New York (2002).
27. Villadsen, J., and Michelsen, M. L., Solution of differential equation models by polynomial approximation, 1st ed., Prentice-Hall, Engelwood Cliffs, New Jersey (1978).
28. Villadsen J., and Michelsen M. L., Selected approximation methods for chemical engineering problems, Reproset, Copenhagen (1970).
29. MATLAB software, The language of technical computing, Math Works Inc. (2006) http: //www.mathworks.com.
30. Pakseresht, S., Evaluation of simulated moving beds performance as a seperative reactor, Ph.D. Thesis, Sharif University of Technology (1999).